

We are IntechOpen, the world's leading publisher of Open Access books Built by scientists, for scientists

6,900

Open access books available

186,000

International authors and editors

200M

Downloads

Our authors are among the

154

Countries delivered to

TOP 1%

most cited scientists

12.2%

Contributors from top 500 universities



WEB OF SCIENCE™

Selection of our books indexed in the Book Citation Index
in Web of Science™ Core Collection (BKCI)

Interested in publishing with us?
Contact book.department@intechopen.com

Numbers displayed above are based on latest data collected.
For more information visit www.intechopen.com



Electron Microscopy in the Diagnosis of Amyloidosis

Tosoni A., Barbiano di Belgiojoso G. and Nebuloni M.
*Pathology Unit and *Nephrology Unit, L.Sacco Dept. Clinical Sciences,
 University of Milan, Milan,
 Italy*

1. Introduction

Amyloidosis defines a pathological condition in which organ and tissue damage is related to the extracellular deposition of amyloid fibrils, deriving from specific proteins, the amyloid precursor proteins. More than 25 different precursor proteins are associated with different forms of amyloidosis, which are summarized in Tables 1 and 2. The modern nomenclature is based on the type of amyloid protein involved (Sipe et al., 2010). A subdivision into systemic and localized amyloidosis is also frequently adopted and is relevant in clinical practice and histopathology (Picken, 2010). However, although certain amyloid forms are exclusively localized (e.g. neurodegenerative A β), others (e.g. AL) can be either systemic or localized. Prions are usually considered a distinct clinico-pathological entity in connection with their peculiar infectious nature.

2. Structural and morphological aspects of amyloid

2.1 Amyloid fibrils structure

Structural definition of amyloid differs from those used for diagnostic purpose (Fandrich, 2007; Greenwald & Riek, 2010). Pathologists define amyloid on the basis of its presentation in pathological tissues, namely: extracellular deposition of protein with characteristic fibrils appearance in electron microscopy -EM-, typical X-ray diffraction pattern and affinity for Congo red with concomitant green birefringence. Secondary components such as serum amyloid P integrate definition of amyloid deposits. By contrast, in molecular structural studies, tissue depositions are less important than structural similarities. In this context amyloid is defined on the basis of the characteristic conformational arrangement of the proteins, consisting in highly ordered cross-beta sheet aggregates. This definition of amyloid includes pathologic amyloid proteins, synthetic peptides or proteins that form amyloid fibrils *in vitro* but are not associated to clinical symptoms, such as glucagon (Pedersen et al., 2010), certain intra-cellular physiological and pathological proteins (e.g. pituitary peptide hormones, tau neurofibrillary tangles in Alzheimer's disease, α -synuclein in Lewy bodies of Parkinson's diseases), and peculiar natural functional proteins such as curli, an *E. coli* biofilm protein (Greenwald & Riek 2010; Pedersen et al., 2010). Most common high resolution structural methods for proteins, such as Nuclear Magnetic Resonance -NMR- in aqueous solution and crystals X-ray diffraction, are not feasible or limited by the intrinsic nature of the fibrils, which

Precursor	Amyloid protein	Disease	Mainly involved organs
Ig k or λ chain	AL	Primary Myeloma associated SA	Kidney, heart, liver, GI, peripheral nerve, soft tissues
Ig heavy chain	AH	Primary Myeloma associated SA	Kidney, heart
Serum apolipoprotein A	AA	Secondary reactive SA	Kidney, GI, liver, spleen, soft tissues
β 2-microglobulin	A β 2M	Hemodialysis related SA	Osteoarticular tissue, heart, GI, lung, soft tissue
Apolipoprotein AIV	AApo AIV	SA associated with aging	Rare forms of SA
Transthyretin	ATTR	Senile SA.	Heart, vessels, soft tissues
Leukocyte chemotactic factor 2	ALect2 rare	SA	Kidney, liver
Mutant fibrinogen α -chain	AFib	FSA	Kidney, liver, spleen
Mutant transthyretin	ATTR	FSA familial amyloid polyneuropathy I	Peripheral nerve, heart, GI, kidney
Mutant lysozyme	ALys	Hereditary non neuropathic SA,	Kidney, liver, spleen, GI
Mutant apolipoprotein AI	AApoAI	FSA familial amyloid polyneuropathy II	Liver, kidney, heart, spleen, peripheral nerve, GI, skin, larynx
Mutant apolipoprotein AII	AApoAII	FSA	Kidney, heart
Mutant gelsolin	AGel	Finnish hereditary SA	Cornea, cranial nerves
Mutant cystatin C	ACys	FSA Hereditary cerebral amyloid angiopathy	Cerebral vessels
Mutant protein of ABri	ABri rare	British Familial dementia	CNS

Table 1. Types of amyloid proteins associated with systemic diseases and different organ involvement. (SA=systemic amyloidosis, A=amyloidosis, FSA=familial systemic amyloidosis GI=gastrointestinal tract, NS= nervous system. Pettersoon 2010, Sipe 2010, Dember 2006)

	Precursor	Amyloid protein	Disease	Organ involved
Localized presentation of systemic form		AL	Localized primary A	Various (kidney, skin, bladder, lymph node, GI)
		AH	Localized primary A	Kidney
		AApoAI	LA	Aortic atherosclerotic plaques, meniscus
Neurodegenerative form with amyloid plaques	A β protein precursor AAP	A β	Alzheimer's disease (sporadic and familial), hereditary cerebral amyloid angiopathy, senile dementia	CNS
	Prions (transmissible amyloid proteins)	APrP	Sporadic (Kuru), new variant (alimentary) and familial CJD, GSSD	CNS
Other forms of LA	Pro-calcitonina	ACal	Tumor associated A	C-cell thyroid tumors
	Amylin - Islet amyloid polypeptide	AIAPP	Tumor associated A	Insulinoma
	Prolactin	APro	Tumor associated A	Prolactinoma
	Mutant protein of ABri and ADan	ADan	Familial dementia	CNS
	Mutant Keratoepithelin	AKer	Familial corneal amyloidosis	Cornea
	Mutant corneodesmosin	ACDSN New ^	A in hypotrichosis simplex of the scalp	Hair follicle, papillary dermis
	Lactoferrin	ALac	Corneal amyloidosis	Cornea
	Keratins	AK	Likenoid and macular A	Skin
	Lactadherin - Medin	AMed	Senile Aortic A	Aorta
	Atrial natriuretic factor	AANF	Atrial A	Cardiac atria
	Seminogelin	ASeml	LA	Vescicula seminalis
	Amylin - Islet amyloid polypeptide	AIAPP	Diabetes type II	Islets of Langerhans
	Prolactin	APro	Aging pituitary	Pituitary gland
	Insulin	AIns	Injection-localized A	Injection-localized

Table 2. Types of amyloid protein associated with localized diseases. (LA=localized amyloidosis, A=amyloidosis, CJD=Creutzfeldt-Jakob Disease, GSSD=Gerstmann-Straussler-Scheinker Disease. Sipe 2010, Merlini 2003, Furnier 2000, ^Caubet 2010, Sikorska 2009)

are insoluble in water and represent one-dimensional forms, with single translational and rotational symmetry elements. The various other technologies employed include: NMR in solid-state, circular dichroism, Fourier transform infrared spectroscopy, atomic force and EM. Currently, high resolution structural data regarding the fibrils of the different types of amyloid remain fragmentary, and frequently they depend on used technical approach (Fandrich, 2007; Sachse et al., 2006; Jimenez et al., 2001; Stromer & Serpel 2005). Most of the current structural data on amyloid fibrils derive from EM such as transmission EM –TEM- techniques, electron-diffraction microscopy, and, more recently, scanning TEM and cryo TEM, using single particle image analysis (Jimenez et al., 2001; Stromer & Serpel 2005). Reports giving models for structure of amyloid fibrils are based mainly on TEM and atomic force diffraction studies of amyloid extracted from tissue and purified (*ex vivo* studies), or synthetic short peptides from amyloid protein sequences (*in vitro* studies). Non fibrillar components of amyloid present *in vivo* are lost during extraction processes or normally absent in *in vitro* experiments. Globally, the data obtained so far outline the following general characteristics of amyloid fibrils (Fandrich, 2007; Jimenez et al., 2001; Makin & Serpell 2005):

- Different protein sequences form fibrils with high structural similarities.
- Amyloid fibrils extracted from tissues or assembled *in vitro*, when observed at medium magnifications, are similar in diameter and general morphology to those observed *in vivo*.
- Fibrils are long, undetermined in length, straight or moderately curved (A β 2M), and generally not branched.
- Amyloid fibrils can appear as wavy filaments, road shaped or twisted, with a diameter ranging from 5 to 25 nm.
- Most types of amyloid fibrils are formed by assembling of fibrillar subunits named “protofilaments”. In mature fibrils, protofilaments can vary in number (2-6) and can twist one another forming an hollow fibril core. Discernible periodicity can arise from twisted and ribbon-like structures of the fibrils.
- Metastable fibrils precursors include protofibrils and non fibrillar aggregate-soluble oligomers.
- Protofibrils are 2-5 nm in diameter, shorter than fibrils, curl and irregular (worm-like) in their overall structure. They contain one or more linear row of the amyloid protein molecules. Some authors use the term protofibrils also for non fibrillar aggregates.
- Mature fibrils and metastable forms of amyloid are all characterized by cross-beta-sheet conformation.
- Observed with high resolution techniques oligomers, protofibrils, protofilaments and fibrils of the amyloid are structurally heterogeneous.
- Structural characters of oligomers, protofibrils, protofilament and fibrils are influenced by: sequence of the protein, concentration, and various other fibrils growth conditions.

The most distinctive structural feature of amyloid is the structural polymorphism of their aggregates and fibrils in *in vitro* and in *ex vivo* experiments. This is found also within the tissue extracted, and even more in experiments *in vitro* under the same conditions of incubation (Pedersen et al., 2010; Fandrich, 2007, 2009). TEM images can demonstrate the variations of degree of twisting, number of protofilaments forming a fibril, and mature fibrils diameter (Fandrich et al., 2009; Greenwald & Riek 2010).

Amyloid may be considered a characteristic structural status of a protein in certain conditions. For this reason amyloidosis is defined a conformational protein disease. In amyloidosis, an amyloid precursor protein, with or without post-transcriptional modifications, sometimes favored by mutations (hereditary amyloidosis), and in particular experimental conditions *in vitro*, can lead to beta-sheet peculiar aggregation, forming insoluble fibrils. Moreover, in prion diseases, an infective prion protein can induce cross beta-sheet conformation and amyloid deposition of the constitutive protein (Pan et al, 1993; Prusiner, 1998). Understanding the structure of amyloid and their formation is the prerequisite for developing methods to rationally interfere in the mechanism of pathologic aggregation responsible for important human diseases.

2.2 Ultrastructural morphology of amyloid fibrils in tissues

In 1959 Cohen and Calkins demonstrated, for the first time, that different forms of amyloid exhibit a comparable fibrillar ultrastructure in fixed tissue sections (Sipe & Choen, 2000). This has been amply confirmed by successive studies, which evidenced that all types of amyloid deposits seen in different tissues, and regardless of the clinical/biochemical form, are mainly composed of bundle of not branched, straight fibrils, ranging from 6nm to 13nm in diameter (average 7,5-10 nm) and 100-1600 nm in length (Sipe & Choen, 2000). Ultrastructural demonstration of this peculiar fibrillar morphology was adopted as one of the criteria for the definition of amyloid. Subsequently, studies on amyloid extracted from tissues, and *in vitro* studies on amyloid proteins synthetic derivates, are the basis of the most of high-resolution structural data regarding amyloid, which are described in the previous paragraph. It must be stressed that these structural data refer to pure, purified or partially purified amyloid proteins. High resolution -HR- structural studies of amyloid in tissues (*in situ* studies) are few and consist mainly in TEM analyses at high magnification (x500000 or more) of thin sections of plastic embedded fixed tissues. Immunolabeling procedures for TEM are applied to distinguish amyloid proteins from other tissue constituents (Inoue et al., 1997, 1998, 1999). Image reconstruction techniques are used for the formulation of the structural models. Structural models deriving from *in vitro* and *ex vivo* experiments are only partially confirmed by *in situ* HR TEM analyses. In fact: amyloid fibrils in tissue appear not branched, rigid, about 10 nm in diameters, but - for example- the substructural organization in protofilaments is rarely described and can be different from that observed in *in vitro* experiments. However, immuno-labeling techniques -including immuno-electron transmission microscopy -ITEM- demonstrated that other various components are present in tissue amyloid deposits (Inoue et al., 1997, 1998, 1999; Sipe & Choen, 2000). These do not form fibrils *in vitro*, but are implicated in amyloid deposition and stability. Non fibrillar components, commonly present in various types of amyloid deposits, include: proteins (serum amyloid P component SAP, apolipoprotein E), proteoglycans -PG- (condroitinsulfate PG, heparansulfate PG) and lipids (Pettersson & Konttinen, 2010; Merlini et al., 2003; Gellermann et al., 2005). These are mostly or partially lost during extraction procedures, and they are not present in *in vitro* experiments. This fact could justify the structural differences of amyloid analyzed *in situ* (Sipe & Cohen, 2000; Inoue et al., 1998). At present, review of morphological studies *in situ* of amyloid deposits (Sipe & Cohen, 2000; Sikorska et al., 2009; Inoue et al., 1997, 1998, 1999; Bely et al., 2005) outlines the following general characteristics:

- In systemic and most of localized forms of amyloidosis, amyloid deposits contain not branched fibrils, from 6nm to 13nm in diameter (average 7,5-10 nm), and variable length.
- In neurodegenerative prion forms, amyloid fibrils diameters range from 7-8 nm -in Kuro plaques- to 17-24 nm -in variant Creutzfeldt-Jakob disease plaques- depending on the sequence mutations of amyloid precursor proteins.
- Diameters of the fibrils depend also on fixation procedure used to prepare the tissues.
- The fibrils are more frequently straight, but curved shapes were also described, especially for A β 2M type.
- At high magnification the fibrils did not appear to be formed by protofilament subunits. They show frequently cross bands along the axis, and a tubular appearance due to an empty core (Fig. 1), a central dense dot is described by Inoue et al. (Inoue et al., 1997, 1998, 1999).
- ITEM analyses with antibodies specific for amyloid proteins identify: non fibrillar-amorphous aggregates, filaments about 0,5-1 nm in diameter, and protofibrils 3-5 nm in diameter, which can be observed close to the fibrils or in their proximity.
- ITEM analyses show that specific antibodies to non fibrillar component of amyloid appear tight to fibrils. This fact is at the basis of Inoue models, in which SAP and PG play a structural role in the construction of the fibrils.

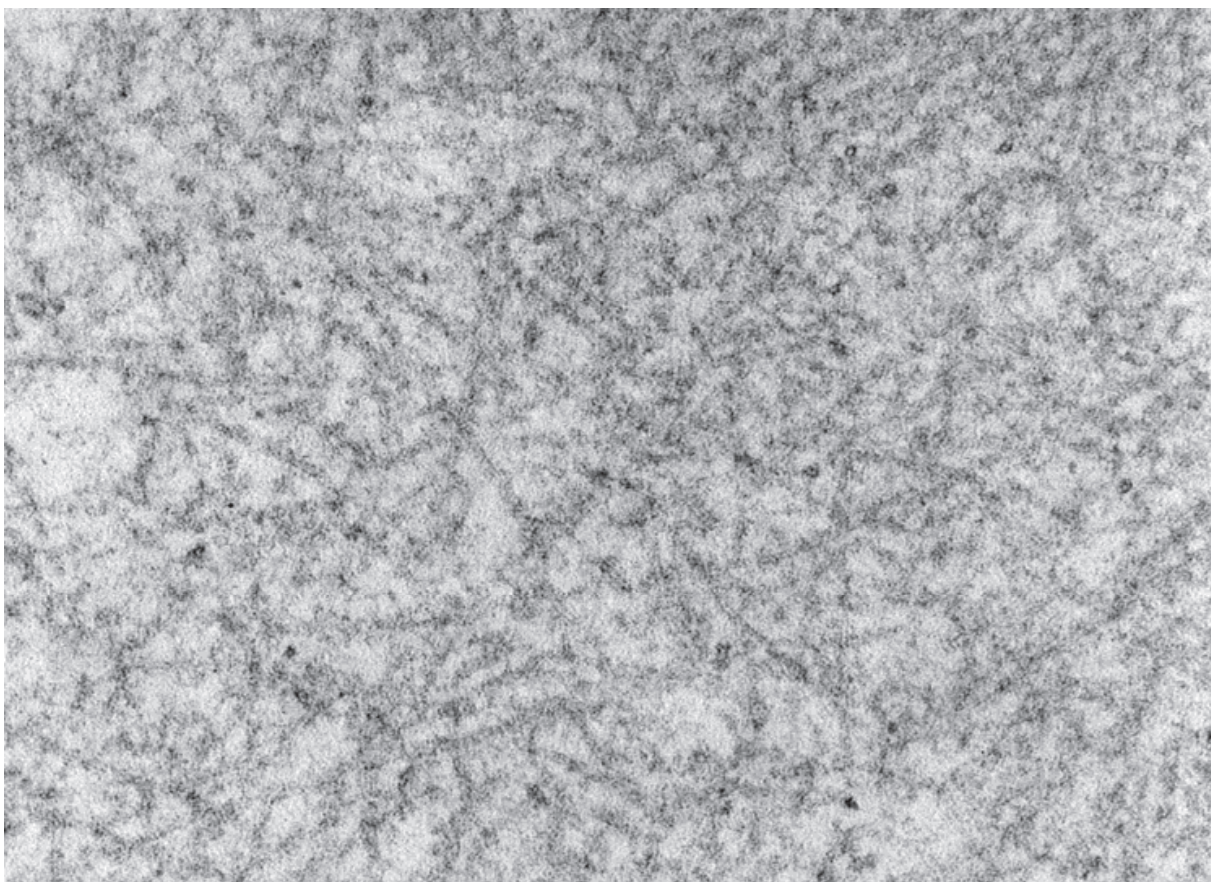


Fig. 1. Amyloid fibrils in a case with AL amyloidosis. At high magnification the fibrils appear straight and non branched. Cross band along their axis and a clear hollow centre can be seen focally. Original magnification -OM- : x50000.

Overall, the morphological definition of amyloid remains the one described by Cohen and colleagues in their first ultrastructural studies. Atypical ultrastructural presentation corresponding to Congo red stained-birefringence tissue deposits must be confirmed as amyloid using ITEM techniques. Additional studies in tissue, using new techniques, are needed to confirm the actual molecular structure of amyloid fibrils *in vivo*.

2.3 Ultrastructural morphology of amyloid deposit in tissue

Ultrastructural analyses of amyloid *in situ* provide additional information regarding arrangement and distribution of amyloid fibrils *in vivo* and their structural interaction with extracellular matrix elements and cells.

The amyloid fibrils tissues aggregates may be in sparse or dense pattern (Fig. 2).

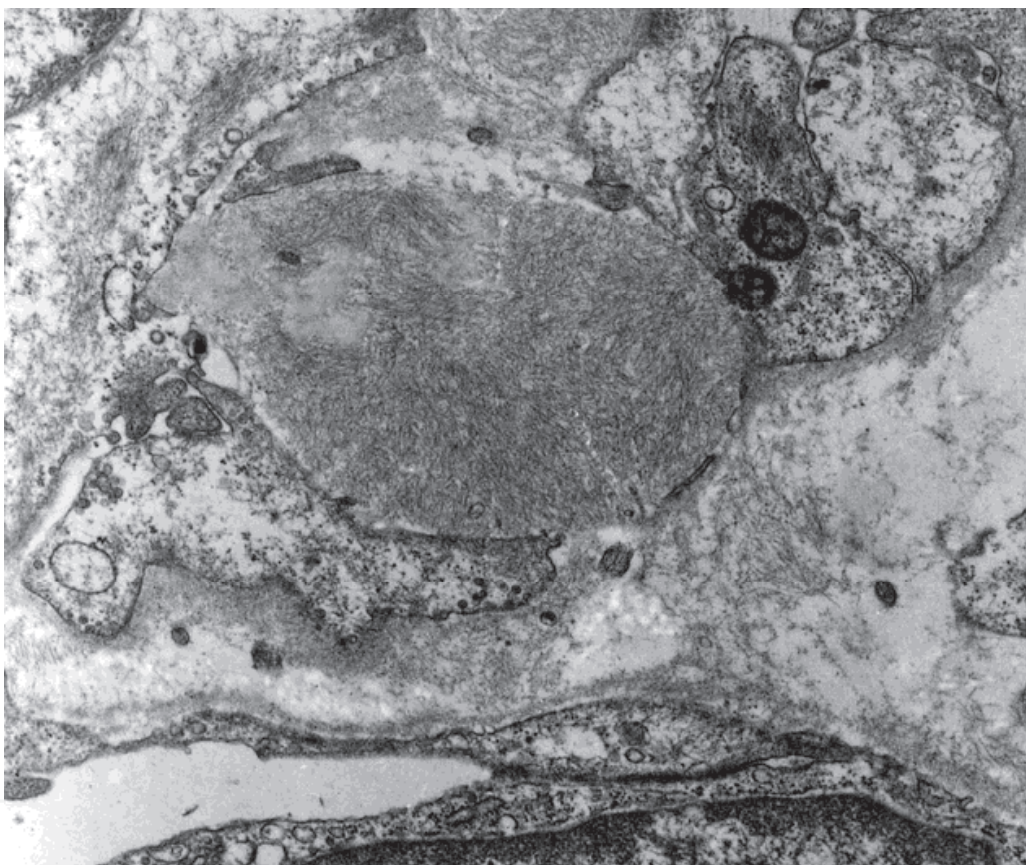


Fig. 2. Dense and few scattered aggregates of amyloid fibrils between pericytes, from a renal biopsy in a case of AL amyloidosis. OM: x7000.

Haphazard arrangement represents the more frequent and specific array of amyloid fibrils in tissues. However, star-like, parallel, and curving arrays are also frequently documented. *In vivo*, amyloid deposit morphology can also change after deposition. In advanced amyloidosis, older amyloid deposits, can appear as dense ovoid-globular aggregates, or inhomogeneous deposits with multifocal accumulation of densely packed short fibrils and filaments. Centre of the dense deposits may be lacking of immunoreactivity for anti-amyloid protein antibodies (Bely et al., 2005). Frequently, distinction of fibrils in dense aggregates is easier at their marginal zone (Nishi et al., 2008). Particular aggregation patterns include glomerular “spikes” and cerebral amyloid plaques.

2.3.1 Glomerular sub-epithelial “spikes”

“Spikes” are a peculiar amyloid fibrils aggregation described in glomerular AA and AL amyloidosis. They consist in fibrils in parallel spicular array, crossing the glomerular basement membrane at the right angle and pointing to the foot processes of podocytes (Fig. 3) (Dickman et al., 1981; Nishi et al., 2008).

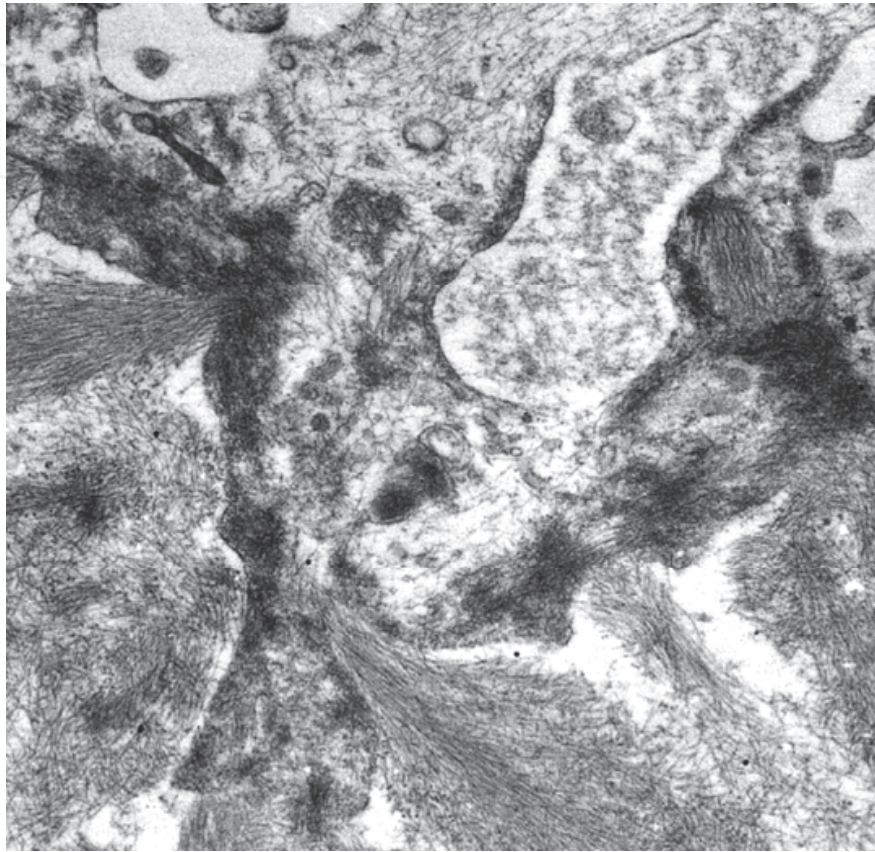


Fig. 3. Spicular array of amyloid fibrils. Under a wide foot process of a podocyte, in a case of AA amyloidosis. OM: x4400.

2.3.2 Cerebral amyloid plaques

Peculiar star-like aggregation of the fibrils are the cerebral amyloid plaques in neurodegenerative diseases due to A β and APr including: Alzheimer’s disease (sporadic and familial), age-related or senile dementia, Sporadic (Kuru), new variant (alimentary) and familial Creutzfeldt-Jakob Disease -CJD-, Gerstmann-Straussler-Scheinker disease -GSSD-. Despite in all these forms neurotoxicity is linked mainly to oligomers of amyloid proteins, presence of amyloid plaque correlate to progression of the disease (Sikorska et al., 2009; Fiedrich et al., 2010; Merlini & Bellotti, 2003). Morphological characters and distribution of amyloid plaques, determined by light microscopy-LM-, differ in the various clinical-pathological forms, and can help the diagnosis. TEM and ITEM studies of amyloid plaques demonstrated that they are ordered aggregates with bundles of fibrils departing radially from a central core. The plaques are located at the neuropil, between glial and neural processes. The different ultrastructural characters described in the different clinical-pathological form (Serpell, 2000; Sikorska et al., 2009; Fournier et al., 2000) are summarized below:

- Classical senile plaques, present also in Alzheimer's disease, are star-like closely packed bundles of A β fibrils forming a generally dense fibrillar core, which is surrounded by dystrophic neuritis, activated microglia, and reactive astrocytes. In Alzheimer's diseases typically plaques are numerous, and present several dystrophic neurites and microglial cells. Senile plaques can be observed also in prion diseases, in addition to prion plaques. In Alzheimer and senile dementia another form of amyloid is present. It is the intracellular cross-beta sheet tau fibrillar aggregates forming neurofibrillary tangles.
- "Kuro" star-like plaques are relatively small, formed by bundles of fibrils mixed to electron dense material and cellular element. Dystrophic neurites are rarely identified. The plaques are surrounded by glial cells (Fig. 4). Jatrogenic CJD plaques are typically enclosed by numerous astrocytes. "Kuro" plaques are present in all forms of CJD. They are more numerous and smaller in jatrogenic CJD. Small Kuro plaques, distributed in clusters, are observed in new variant CJD (alimentary).
- Florid plaques of new variant CJD: amyloid plaques contain and are surrounded by vacuoles deriving from swelled cell processes. The radially arranged bundles of fibrils are very thick. They are loosely mixed to non fibrillar prion proteins, swollen glial and neural cell processes, and numerous dystrophic neurites with synaptic elements. Numerous microglial cells, sometimes with intracellular fibrils in vacuoles, are present around and within the plaques.
- GSSD multicentric plaques: bundles of fibrils depart radially from more than one central dense core, dystrophic neurites are mixed to fibrillar amyloid bundles. Microglial cells are also observed.

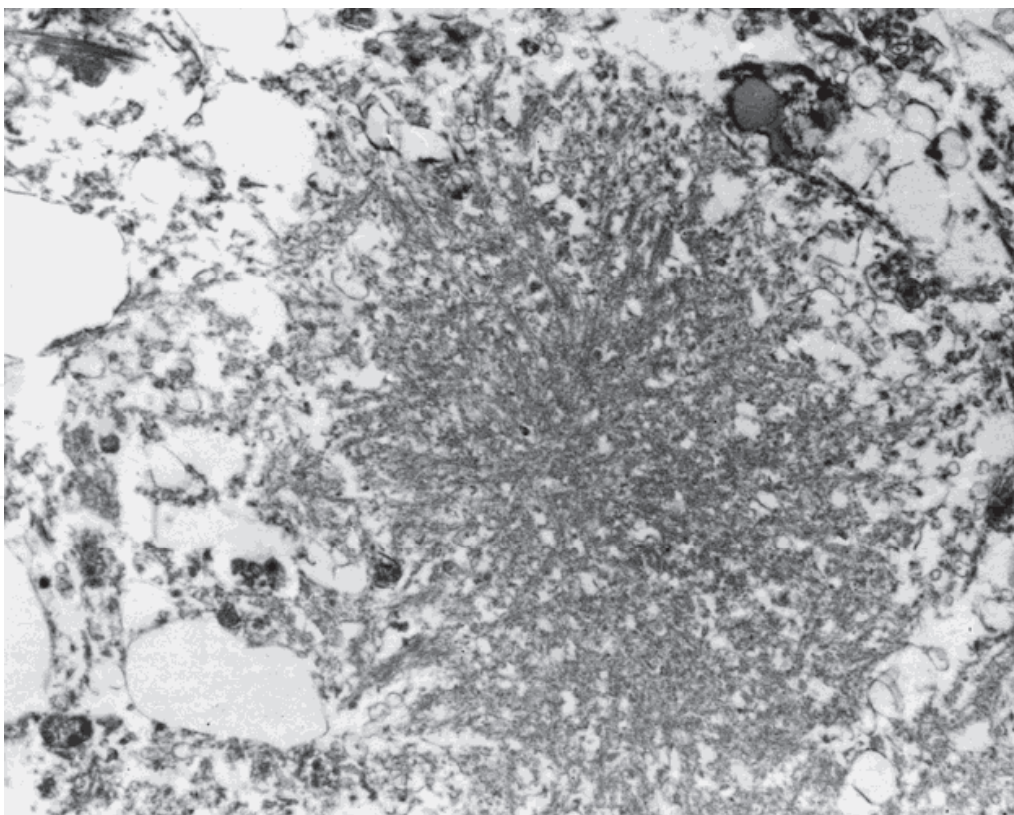


Fig. 4. A small Kuru-like PrP plaque, with bundles of filaments in a star-like array. Amyloid bundles are mixed with scattered electron-dense material. OM: x3000.

A β and APr fibrils are also present in haphazard arrangement in the “diffuse plaques” more frequently observed in Alzheimer’s diseases associated to Down syndrome and in hereditary cerebral amyloid angiopathy (Allsop et al., 1986; Rozemuller et al., 1993; Yamaguchi et al., 1989). Diffuse plaques are not associated to neuritic alterations. They contain a scanty amount of fibrils, and can be negative at Congo red stain and birefringence. These amyloid deposits are evidenced mainly by immune-labeling, and using methenamine silver staining methods. TEM studies in Alzheimer’s diseases describe also the presence of small clusters of randomly arranged fibrils associated to neurite degeneration. These are retained primitive A β classical plaque forms. Perivascular non ordered amyloid fibrils are frequently identified in neurodegenerative amyloidosis but they are the prevalent amyloid deposition in prion associated hereditary cerebral amyloid angiopathy. The described morphological differences of cerebral amyloid deposits in neurodegenerative amyloidosis demonstrate a different fibril distribution and different cells injury and reaction, depending from amyloid protein sequence and mutations.

2.4 Intracellular amyloid fibrils in amyloidosis

Amyloid fibrils are frequently reported within lysosomes of reticuloendothelial or macrophage system cells (including microglia and glomerular mesangial cells), in proximity to amyloid deposits (Sikorska et al., 2009; Bely et al., 2005; Santostefano et al., 2005; Keeling et al., 2004; Kluge-Beckerman et al., 1999; Morten et al., 2007). The presence of amyloid within phagocytes *in vivo* remains controversial. It can derive from the capture of extracellular amyloid by phagocytosis for degradation. This may indicate a protective role of macrophages activity. However, resistance to lysosomal proteases has been observed for A β 2m, AAmylin, A β , prions, and it may be a generic feature of amyloid. Amyloid could be produced within macrophages. Phagocytes could promote fibrils self-assembling within their endosome or lysosome compartments, favoring protein precursor concentration or modifying protein conformation within acidic endolysosomal compartments. They also could be involved in proteolytic cleavages, producing protein fragments with increased amyloid propensity. Phagocytic cell lines cultured *in vitro* have been shown to promote the fibrillar aggregation of Ig light chains proteins and serum apolipoprotein A (Kluge-Beckerman et al., 1999; Keeling et al., 2004; Santostefano et al., 2005; Friedrich et al., 2010; Teng et al., 2004; Yazawa et al., 2001). At present, data regarding amyloid and their biogenesis *in vivo* remain limited, especially those referred to the structural aspects in extracellular spaces and distribution within the cell compartments. Most of the data regarding fibrillogenesis derive from studies of cell lines cultured *in vitro*, which frequently include ITEM approach (Leonhardt et al., 2010). An increase in the knowledge on endosomal and lysosomal system involvement in amyloid genesis can guide drug discovery of new therapeutic agents.

3. Diagnostic TEM in amyloidosis

The importance of an early diagnosis of amyloid and the correct typing of fibrils have been realized in order to recent advances in the treatment of systemic amyloidosis (Picken, 2010; Pettersson & Kontinen, 2010). No diagnostic biochemical markers in body fluids are known to date. APr and A β neurodegenerative amyloid forms are mainly clinically diagnosed. When autopsy confirmation is required, it is relied on histochemical characterization, and

immunohistochemical and biochemical typing. For the other forms of amyloidosis, the diagnosis consists in the detection and typing of deposits in tissue biopsies or needle aspirates. In the latter context, the ultrastructural analyses are used in first steps of detection of amyloid, together with polarized LM on Congo red stained sections. Congo red staining and birefringence detection are considered to be the gold standard techniques for the demonstration of amyloid deposits. However, specificity and sensitivity of this technique may depend on the experience of the observer, fixation procedure, section thickness, proper staining protocol, and appropriate optics (Picken, 2010). Ultrastructural analysis is particularly useful in early amyloid deposition. In these cases amyloidosis might not be evident at LM because fibrils deposition is minimal and Congo red staining is negative. Moreover, ultrastructural appearance of amyloid may be important in the differential diagnosis of various organized immunodeposits responsible for various forms of glomerulopathies (see upcoming paragraph) and neuropathies (Vallat et al., 2007). However, we should remember some limits of TEM analyses. These are frequently performed on a very small piece of tissue, resulting in a limitation in sensitivity when amyloid deposits are focal and irregularly distributed. The second limit of TEM is that all types of amyloid fibrils have similar morphology. A correct typing of amyloid requires the use of immunolabeling techniques. Unfortunately, the procedures used to preserve morphology at high resolution generally reduce antigens preservation, therefore, amyloid typing is preferably carried out on frozen sections or on formalin fixed paraffin embedded sections. On the other hand, some easy pretreatment of thin sections (e.g. incubation of epon-embedded sections with hydrogen peroxide or periodate solution, or embedding in hydrophilic resins) can ameliorate ITEM results (Inoue et al., 1997, 1998). Ultrastructural localization of amyloid -when possible- increases the sensitivity of the detection, and, above all, ITEM can add important informations for unusual types of amyloidosis (Arbustini et al., 2002; Inoue et al., 1997, 1998, 1999, Caubet et al., 2010). TEM techniques, in tissues and *in vitro*, are frequently included in studies defining new varieties of amyloid (Caubet et al., 2010).

3.1 Systemic amyloidosis

Systemic amyloidosis -SA- represents the most important form of amyloidosis (Pettersson & Konttinen, 2010; Picken, 2010). They comprise a biochemically heterogeneous group of potentially lethal disorders. The main types of SA include, in order of their prevalence: AL, AA, and familial forms. A more recently described form includes dialysis related A β 2m (Jadoul et al., 2001; Bely et al., 2005). An early and specific diagnosis is crucial for the treatment and prognosis. Amyloid deposition can occur in any organ and tissue. For the detection of amyloid, the biopsy of a clinically affected organ is the most sensitive method and may also detect concomitant diseases. The most frequently involved organs correspond to the most frequent diagnostic localization of amyloid. These include kidney, gastrointestinal tract, heart and liver (Pettersson & Konttinen, 2010). Amyloid is frequently reported also in skin in systemic or localized form (Schreml et al., 2010), and in nerve biopsy in cases with neuropathies (Vallat et al., 2007). Certain symptoms in the context of chronic inflammation diseases, plasma cell dyscrasia or familial history, arouse a clinical suspicion of "amyloid syndrome" (Pettersson & Konttinen, 2010). These include mainly proteinuria or renal failure, enteropathy with malabsorption and bleeding, restrictive cardiomyopathy with thromboembolism due to neuropathy, hepatomegalia and

splenomegalia. Some clinical manifestations are more common in certain types of amyloid, but a large variability of presentation is common. In the past, diagnosis of SA in clinically suspected cases was based on rectal and gingival or salivary gland biopsies examination. Currently, abdominal fat needle aspiration or, better, biopsy, are retained the gold standard to confirm the clinical suspicion of systemic amyloidosis. In most cases the samples are completely designed for histopathological analyses and typing (Picken, 2010). However, when a fragment for ultrastructural analyses is disposable, amyloid deposit can be observed in semithin blue stained sections examined by LM as extracellular accumulation of weakly stained material, more frequently in perivascular localization, similar to sclerotic changes. At TEM analysis, amyloid fibrils can be demonstrated in perivascular deposits (Fig. 5A, 5B) and in extracellular matrix deposits, with high sensitivity. It must be stressed that even in cases with a single symptomatic organ involvement with locally demonstrated amyloid deposits, a systemic form must be carefully excluded. In fact, at present the management of localized amyloidosis is mainly conservative where SA involves more radical approaches, including chemotherapy (in AL) and liver transplantation (in familial amyloidosis) (Westermarck et al., 2006; Arbustini et al., 2002; Picken, 2010).

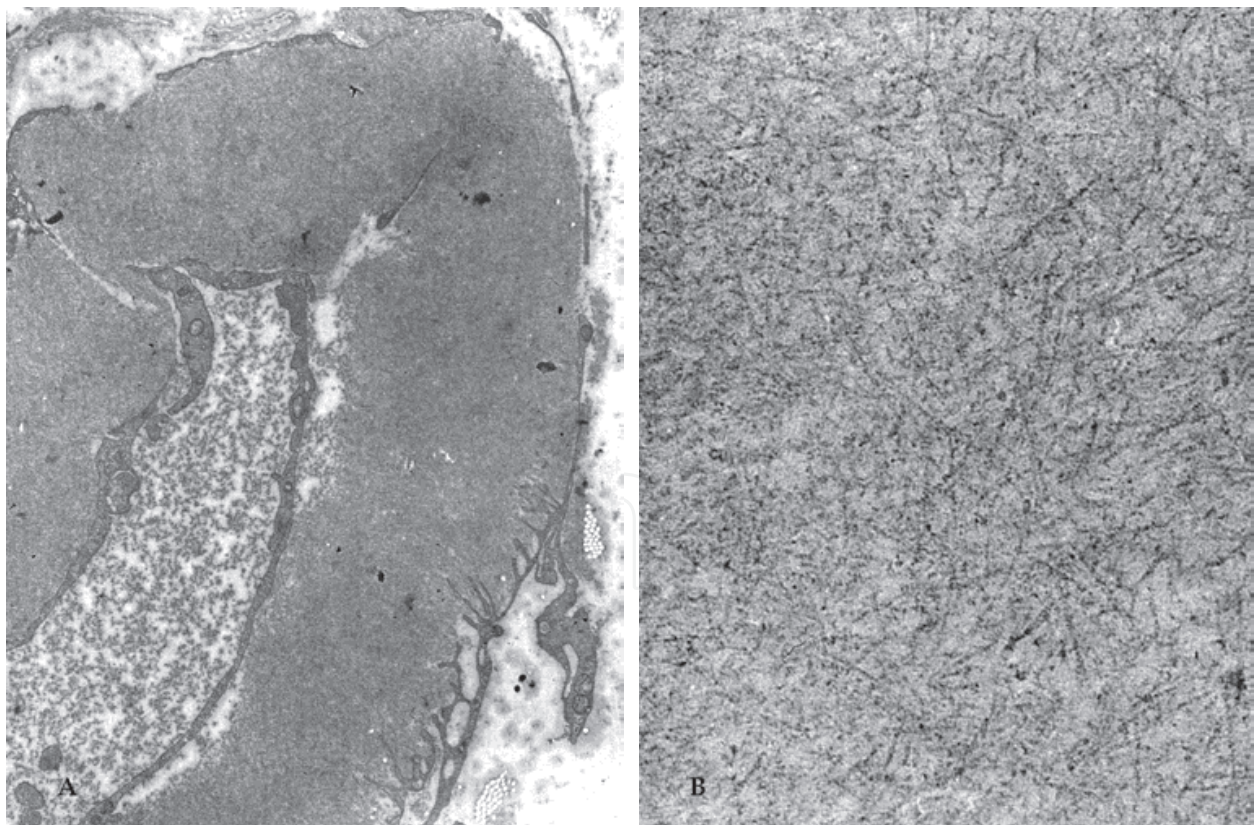


Fig. 5. A-B. Perivascular deposits (A) consisting in amyloid fibrils in haphazard arrangement (B). OM: A. x3000, B. x7000.

3.2 Renal amyloidosis

Among various involved organs in SA, kidney is the most frequently affected (Picken, 2010, Pettersson & Konttinen 2010). In the differential diagnosis of the glomerulopathies, TEM analyses are normally included. Therefore, renal amyloidosis is frequently documented by ultrastructural evidence of fibril deposits.

3.2.1 Clinical presentation

Proteinuria is the clinical manifestation that is present in the majority of patients with renal amyloidosis (Dember, 2006). Ranges of proteinuria are from subnephrotic to massive, with urinary protein excretion rates up to 20-30 g/day. Hypoalbuminemia can be profound, edema is often severe. The level of protein excretion in AL type has been referred to be higher than in AA type, whereas the count of red cells in the sediment significantly higher in AA type, compared to AL type. When amyloid is confined to tubulo-interstitium or vessels, proteinuria can be minimal and reduced renal function is the main clinical manifestation. Renal impairment tends to progress more rapidly when glomerular deposition predominates over tubular and interstitium involvement. Hypertension is an uncommon feature, except when amyloid deposition is relevant in vessels. An unusual manifestation of renal amyloidosis is nephrogenic diabetes insipidus, caused by amyloid deposition in the peri-collecting ducts tissue. Fanconi's syndrome is another extraglomerular manifestation, due to injury to proximal tubular cells by filtered light chains. Amyloid deposits that are isolated to renal medulla is a feature in most patients with ApoAI familial amyloidosis, and has been described in some patients with AA amyloidosis (Nishi et al., 2008; Picken & Linke, 2009). Medullary-limited disease can elude pathologic diagnosis if the biopsy specimen is limited to renal cortex. In synthesis, proteinuria, renal insufficiency, large echogenic kidneys are clinical manifestations that can suggest the suspicion for a renal amyloidosis, which prompts a kidney biopsy (Dember, 2006).

3.2.2 Diagnosis of renal amyloidosis

Amyloid can be found anywhere in the kidney, but glomerular deposition predominates. However, in a small number of cases glomerular deposits are scanty or absent and the amyloid is confined to tubuli and interstitium or vessels (Dember, 2006; Picken & Linke, 2009; Sen & Sarsik, 2010). Glomerular amyloid appears at LM eosinophilic amorphous material in the mesangium and along capillary walls. Periodic acid-Schiff -PAS- staining is weak over nodules, which can be observed in mesangial areas and represent amyloid deposition. Immunofluorescence -IF- on frozen tissue, normally used for diagnosis of immunocomplex glomerulopathy, can be positive for a single light chain isotype, more often lambda chain, in AL amyloidosis, and it can be positive for fibrinogen in cases with AFib. Nevertheless, negative kappa or lambda chain does not exclude AL disease, and a positive immunolabeling does not prove amyloid deposition. The histological diagnosis of renal amyloidosis can be established using Congo red staining, and TEM. Ultrastructural analyses are very useful to identify scanty amyloid deposition in early stages of the disease. Ultrastructural main characters of renal amyloidosis are reported as follows:

- Glomerular amyloid: in the majority of amyloid forms, fibrils are localized preferentially within glomeruli, in mesangial matrix, and basal membranes. The progression of amyloid deposition is associated to mesangial matrix and basal membrane degradation and replacement by amyloid fibrils (Teng et al., 2004). Peculiar spicular aggregates under podocytes foot process, named “spikes” or “spicules” (Dickman et al., 1981; Nishi et al., 2008), are frequently associated to detachments of visceral epithelial cells (Fig. 6). Sub-epithelial “spikes”, when prominent, are visualized also by LM using PAS or methenamine silver stains, which are unusual stains for amyloid. The spikes are generally considered a sign of active fibrils deposition and a bad prognostic parameter (Dickman et al., 1981).
- Extraglomerular amyloid: tubulo-interstitial and vascular deposition can accompany glomerular amyloidosis or characterize certain forms without glomerular involvement. Fibrils can be localized within tubular basal membrane (Fig. 7), in interstitial spaces, and within arteriolar walls.

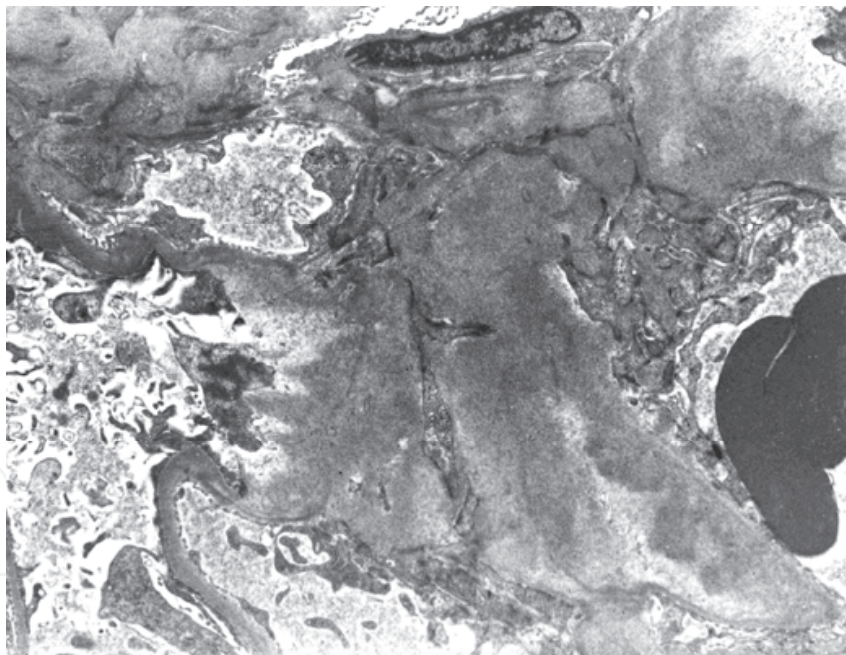


Fig. 6. Massive amyloid deposition and spicular aggregates associated with detachment of visceral epithelial cells. OM: x3000



Fig. 7. Amyloid fibrils within tubular basal membrane and in extracellular matrix. OM: x12000

3.2.3 Histopathological classification and clinicopathological correlations

Though recent reports demonstrated a toxic role of amyloid precursor proteins in AL and AA, amyloid progressive accumulation play an important role in mechanism of renal dysfunction, causing glomerular disruption and also whole renal architecture alterations (Sen & Sarsik, 2010). Most patients with AA or AL disease have predominantly glomerular deposition, and therefore pathologists tried to classify different patterns of glomerular amyloid deposition, in an attempt to quantify the renal damage and to predict patient outcome, depending on severity of glomerular involvement. Dikman et al (Dikman et al., 1981) identified 4 different patterns of glomerular deposition: segmental, diffuse, nodular and mixed, nodular and diffuse. In fact, early glomerular amyloid deposits tend to be spotty and segmental, and late amyloid deposits become more uniform and diffuse. Six patterns or classes of renal amyloidosis were recently proposed by Sen and Sarsik (Sen & Sarsik, 2010), similarly to the systemic lupus erythematosus glomerulonephritis classification. Similarly, this classification of renal amyloidosis is based exclusively on glomerular pathology. Class I, is defined as minimal amyloidosis, with less than 10% extension of glomerular amyloid deposition. The minimal deposition is focal and segmental, within the vascular pole or mesangium. Congo red may not clearly identify the small amyloid deposits. TEM might be necessary for a definitive diagnosis. Definition of the classes, II, III, IV and VI, is based on extension of amyloid deposition within the glomeruli and on the total percentage of involved glomeruli. Class V, or membranous amyloid deposition, i.e. diffuse membranous pattern define a fibril deposition in glomerular basal membranes without prominent mesangial amyloid deposition. This last pattern is mostly associated with AL or non-AA amyloidosis.

Starting from class II, tubulointerstitial and vessels alteration may accompany glomerular lesions. A score of severity, or renal amyloidosis prognostic score-RAPR-, has been proposed by the same authors, taking into account the sum of above described amyloid histological classes, plus global glomerular sclerosis, inflammatory interstitial infiltration, interstitial fibrosis, and tubular atrophy. This severity score is divided into 3 grades: early, late, advanced amyloidosis. The authors applied the new classification and grading system on renal biopsy from patients with AA associated to familial Mediterranean fever, demonstrating a positive correlation between severity of glomerular amyloid deposition, interstitial fibrosis, and inflammation. However, demonstration of a correlation between RAPR and clinical presentation and prognosis are not demonstrated by the authors, and require further studies (Sen & Sarsik, 2010; Dember, 2006). In various classification systems, TEM is fundamental in the definition of class defining minimal amyloid deposition. Sen and Sarsik classification takes into account, and reviews, specific differences in fibrils distribution, depending on the amyloid form, based also on ultrastructural analysis especially for class I definition. These are briefly reported as follows:

- In early AA amyloidosis glomerular fibrils deposition are focal or segmental, within the vascular pole or mesangium. At this stage, in most cases there are no extraglomerular amyloid deposits, except rare cases with only interstitial and vascular deposition.
- In AL, glomerulopathy amyloid tends more frequently to involve capillary basal membrane, also in early stage, frequently with sub-epithelial spikes. Extraglomerular amyloid is of later onset, it is more frequently observed in medulla, and generally it is less important than glomerular deposition.
- Familial renal amyloidosis due to mutant fibrinogen α -chain -AFib - , involve strongly and exclusively the glomeruli. Tendency to amyloid deposition within the basal membrane of the capillary loops is similar to that described in AL.
- In familial renal amyloidosis due to mutant apolipoprotein AI -AApoAI-, amyloid is present only in medulla.
- In transplanted patients with recurrence, and at the same time in patients with AA and rheumatoid arthritis, amyloid may be found only in vascular wall, without glomerular involvement, causing hypertension, which is unusual in amyloidosis presentation.

It must be stressed that a negative detection of amyloid in glomeruli does not exclude a renal amyloidosis: fibrils must be searched carefully also in interstitium, in peritubular basal membranes, and arteriolar walls. Moreover, medulla should be included in the biopsy to identify AApoAI, and some cases of AA.

3.2.4 Renal amyloid typing

The difference in renal distribution of the fibrils may explain different clinical presentation (Dember, 2006), but it is not sufficiently specific to distinguish the amyloid type. IF normally used for diagnosis of glomerulopathy can identify AL light chains or AFib fibrinogen. Other amyloid forms are specifically determined mainly by immunolabeling techniques on paraffin sections and by IF on frozen sections. ITEM is a high sensitive approach to identify and typing the fibrils (Fig.8). However, in a part of cases with AL, commercially available reagents do not always detect the amyloid, because of conformational change or

fragmentation of amyloidogenic light chains, which masks or deletes significant epitopes (Dember, 2006). In cases with negative immunostaining for AL, AA, and more common familial amyloid forms (AFib, ATTR), TEM amyloid deposits demonstration can diagnose amyloidosis or confirm a positive Congo red stain and birefringence analyses. These data, including TEM, justify the demand of additional specific typing tests in specialized institutions. Molecular identification of amyloid protein using proteomic methods such as microextraction and sequencing or tandem mass spectrometry are currently being testing (Picken, 2010).

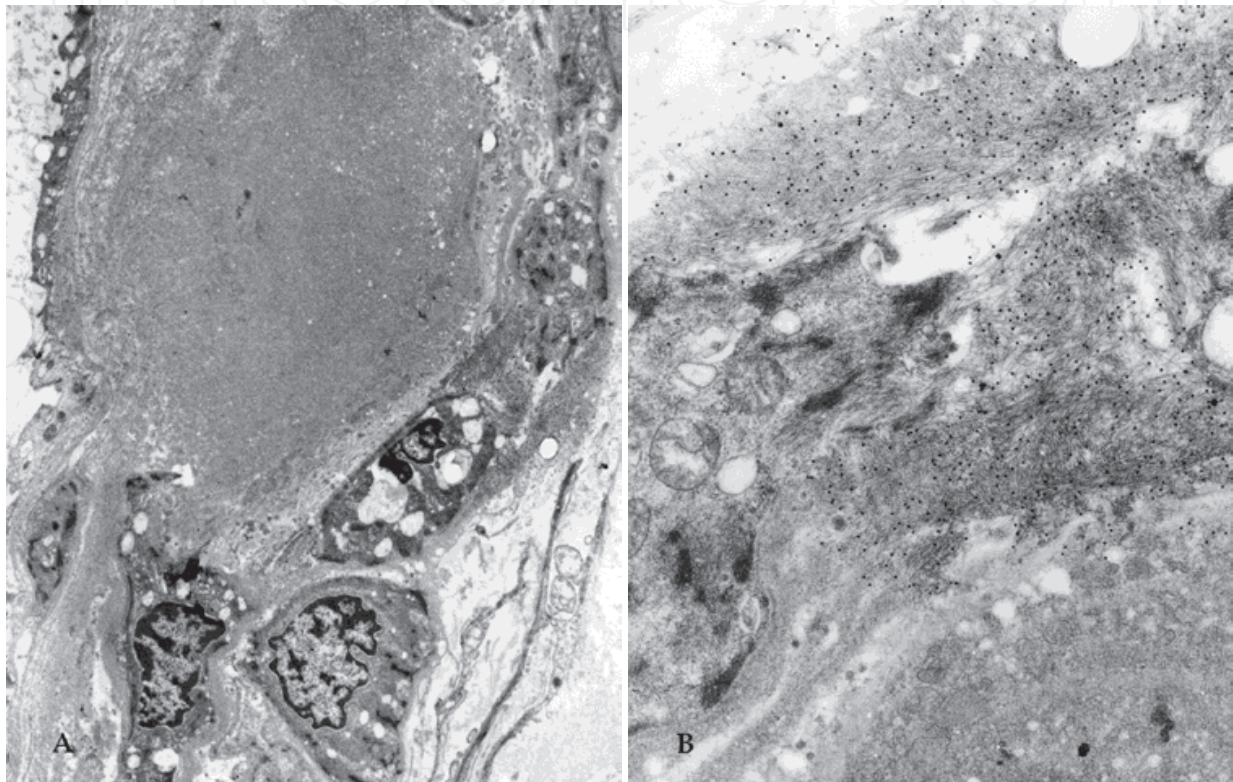


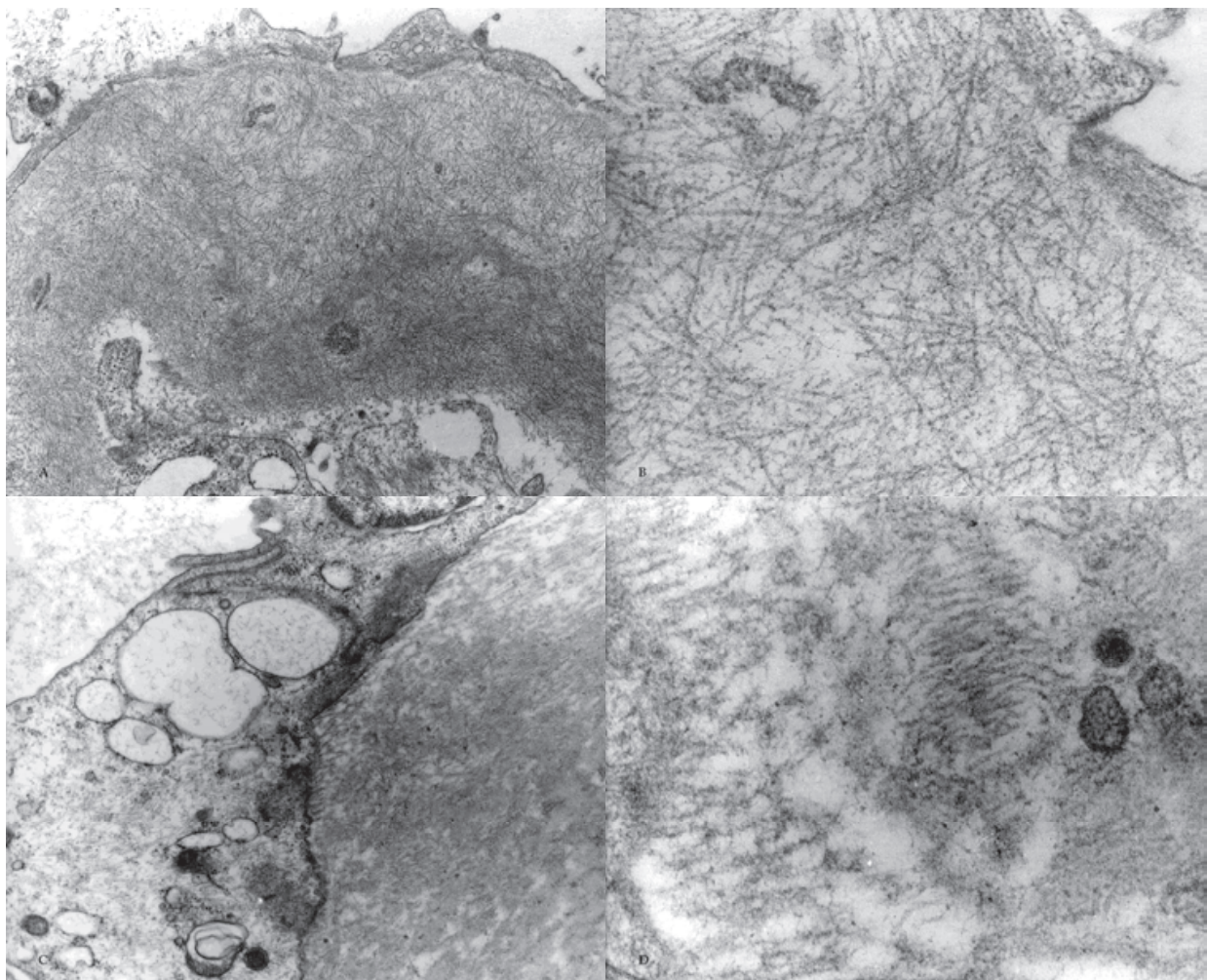
Fig. 8. A-B. Amyloid deposits in the vascular wall of a renal arteriolar vessel (A, OM: x3000). AA amyloid is demonstrated by immuno-gold technique for electron microscopy (B, OM: x12000) (mouse anti human amyloid A monoclonal antibody, DakoCytomation, 1:100 dilution; biotinated rabbit anti mouse as secondary antibody, Dako; immunogold 20nm conjugate streptavidine, British Biocell Int.)

4. Differential diagnosis by TEM analyses

4.1 Non amyloid tissue fibrils in normal and pathologic condition

Specificity and sensitivity of the TEM analyses for amyloid diagnosis are influenced by the presence of the fibrillar components of the extracellular matrix -ECM- in interstitium and basal membranes. Fibrillar ECM comprises fibrils or microfibrils, not branched, straight and with a diameter about 10 nm. These components of ECM similar to amyloid include collagen microfibrils, fibrillin, and fibronectin (Inoue et al., 1999; Kronz et al., 1998; Sherratt et al., 2001; Weber et al., 2002; Dzamba & Peters, 1991). In our experience, basically, amyloid fibrils are more frequently in haphazard arrangement, generally they appear more straight,

better defined, and more electrondense than extracellular matrix fibrils (Fig. 9). The distinction of the different fibrils can be difficult in presence of fibrotic changes in various pathological conditions (e.g. trasplant glomerulopathy, focal glomerulosclerosis, hypertension, mesangiocapillary glomerulonephritis) and particularly in patients with diabetes (Inoue et al., 1999; Kronz et al., 1998). In these latter, the amount of fibrillar ECM increases, and connective fibrils appear more distinct and electrondense. However, ECM fibrils remain mostly in bundle arrays, even if random orientation is focally observed. In uncertain cases with negative Congo red and immunohistochemical staining, ITEM techniques may help a specific distinction. Glomerular normal ECM fibrils include not branched fibrils about 10 nm in diameters in mesangium and, in lesser amount, within basal membrane (Inoue et al., 1999; King et al., 2000). Congo red negative mesangial fibrils about 5-20 nm may commonly be seen in sclerosing glomerular diseases and represent a non specific reaction to glomerular injury (Kronz et al., 1998). These fibrils localize usually in a segmental fashion and are more bundle-like than random arranged. Non-amyloid fibrillar deposit has been frequently described associated to diabetic condition, phenomenon called diabetic fibrillosis. This is characterized by a large amount of not branched mesangial fibrils, and bundles of subendothelial and intramembrane fibrils, with reported diameters ranging from 7 to 16, but they are in average generally wider than amyloid fibrils (King et al., 2000; Korbet et al., 1994; Inoue et al., 1999; Kronz et al., 1998).



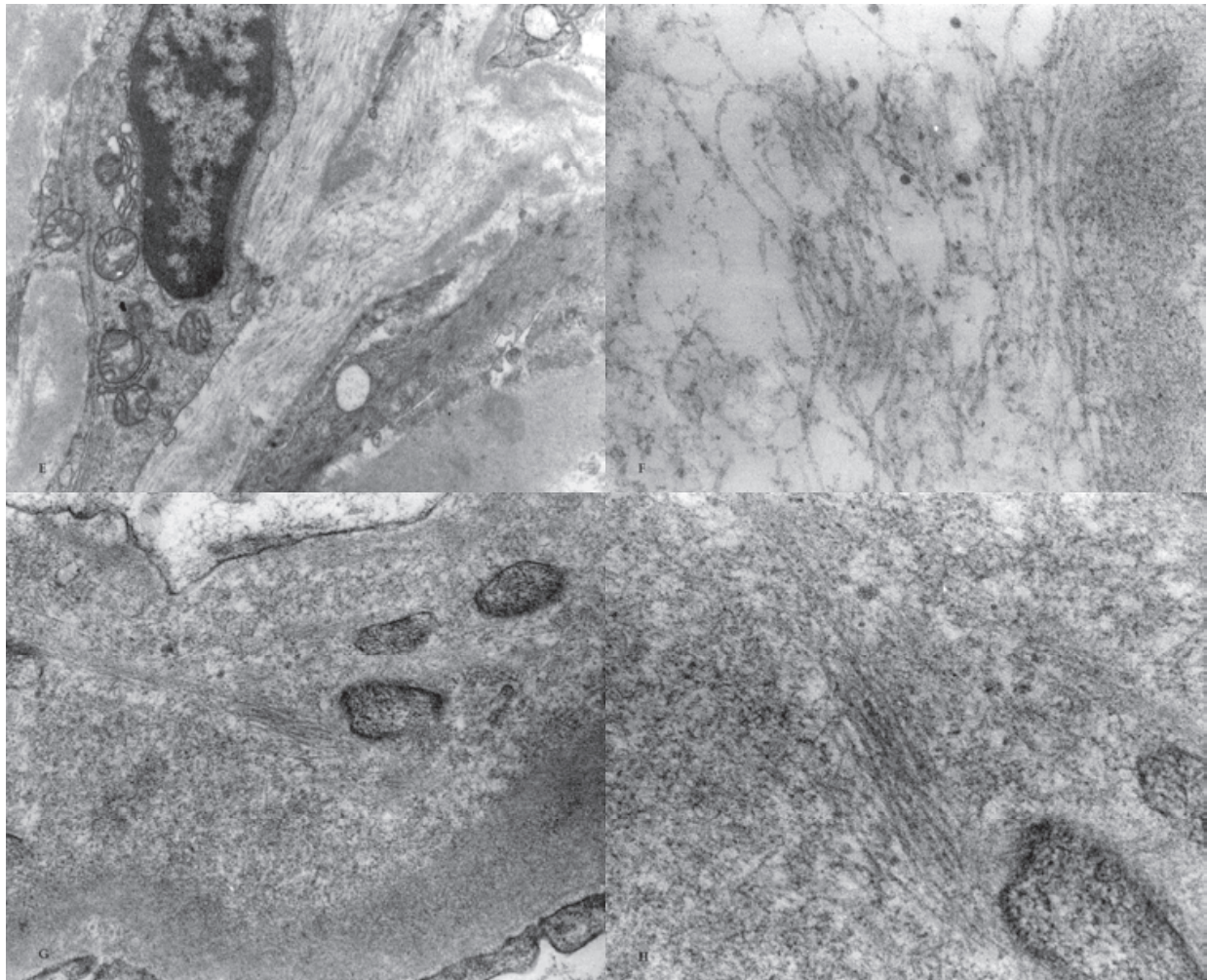


Fig. 9. A.-H. Amyloid (panels A and B) and non amyloid extracellular fibrils (panels C-H). Amyloid deposition in basal membrane of a glomerular capillary is compared with the more ordered array of fibrillin forming endothelial anchoring and stromal fibrils (panels C and D), interstitial fibrillar ECM associated with sclerotic changes (panels E and F) and glomerular sudendothelial fibrils in a case of diabetes. (Panels A, C OM: x12000; Panel E OM: x3000; Panel G OM: x20000; Panels B, D, F, H OM: 50000)

4.2 Disease with structured immunecomplex deposits

Ultrastructural demonstration of amyloid may be important in the differential diagnosis of various organized immunedeposits, responsible for various forms of glomerulopathies and neuropathies (Joh, 2007; Vallat et al., 2007). Fibrils of a wide variety of size and patterns can be seen in the kidney of patient with monoclonal immunoglobulin diseases, lupus nephritis, cryoglobulinemia, collagen III deposition glomerulopathy, hereditary fibronectin nephropathies and immunotactoid glomerulopathy. Structured immunecomplex deposits include: cryoglobulins, finger prints, and fibrillary-immunotactoid deposits (Joh, 2007; Vallat et al., 2007; King et al., 2000). Their main characters and ultrastructural morphology are summarized below:

- *Cryoglobulin deposits* consist in peculiar monoclonal or polyclonal immunoglobulin responsible of cryoglobulinemia. In tissue, their various morphological shapes include: anular, fingerprint-like, microtubular, and microfibrillar shape, with a diameter ranging

from 8 to more than 60 nm. Generally, the structure appears almost indistinct and frequently associated with non-structured deposition. The more typical morphology consist in short tubules, curved and often coupled, about 25 nm in diameters (Fig. 10). These are more frequently observed in cases with mixed (IgM-IgG) essential cryoglobulinemia or type II cryoglobulinemia. They are associated to glomerulopathy (Joh, 2007) and polyneuropathy (Vallat et al., 2007). Glomerular cryoglobulin deposits localize mainly in sub-endothelial lamina rara, with a tendency to form pseudothrombi. They are frequently associated to endocapillary mononuclear infiltrates.

- *Finger-print*: are structured immunecomplex deposits consisting in curved lamelled aggregates with a finger print-like aspect (Fig. 11). They are considered highly suggestive of lupus nephritis and are present in cases with monoclonal dysglobulinemia and polyneuropathy (Joh, 2007; Vallat et al., 2007).
- *Fibrillar and microtubular immunotactoid*: immunecomplex deposition consisting in fibrillar/microtubular aggregation, containing mainly immunoglobulin IgG and complement C3, are respectively associated to fibrillary glomerulonephritis -FGN- and immunotactoid glomerulopathy -ITG- (King et al., 2000; Schwartz et al., 2002; Alpers & Kowalewska, 2008). Immunotactoid fibrillar/tubular structures have a variable diameter ranging from 9 to 60 nm or more, depending on single case (Fig.12). A lucent center, the lumen, is easily identified in microtubules with diameters of 30 nm or more, but higher magnification can demonstrate a lucent centre in all immunotactoid structures independently by their diameters. In ITG, immunotactoid is conventionally defined as deposits of microtubular structures with a diameter greater than 30 nm (mean range 30-60 nm). A larger diameter is associated to the tendency at a parallel arrangement that contribute to define tubular immunotactoid. In FGN, fibrillary form is conventionally defined by presence of Congo red negative deposits of not branched elongated fibrils, more frequently without evidence of a clear centre at median magnification, with a diameter smaller than 30nm and, in some cases, overlapping the amyloid fibrils diameter. Fibrils of FGN, as well as amyloid, typically present a random array of the fibrils.

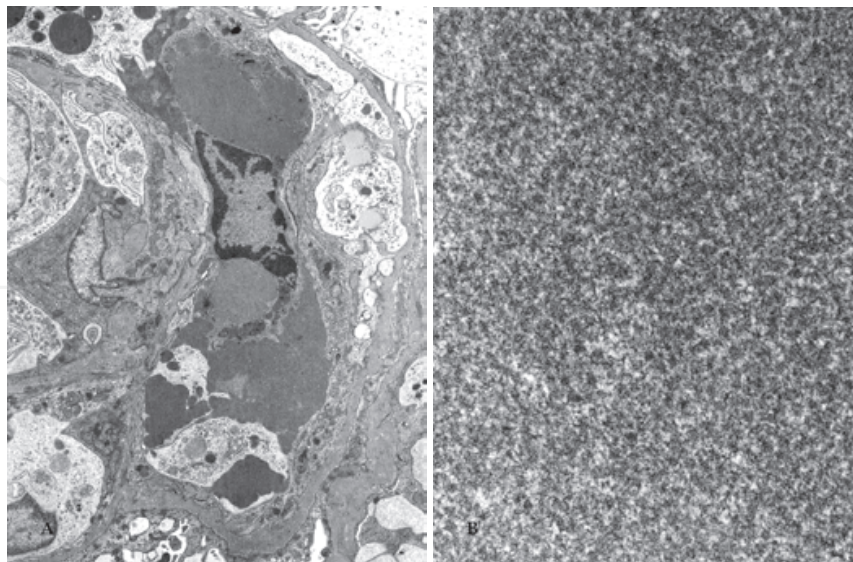


Fig. 10. A glomerular pseudo thrombus (A, OM: x3000) due to cryoglobulin deposition. At high magnification (B, OM: x30000) , the typical structure consisting in curved and often coupled short tubules is shown.

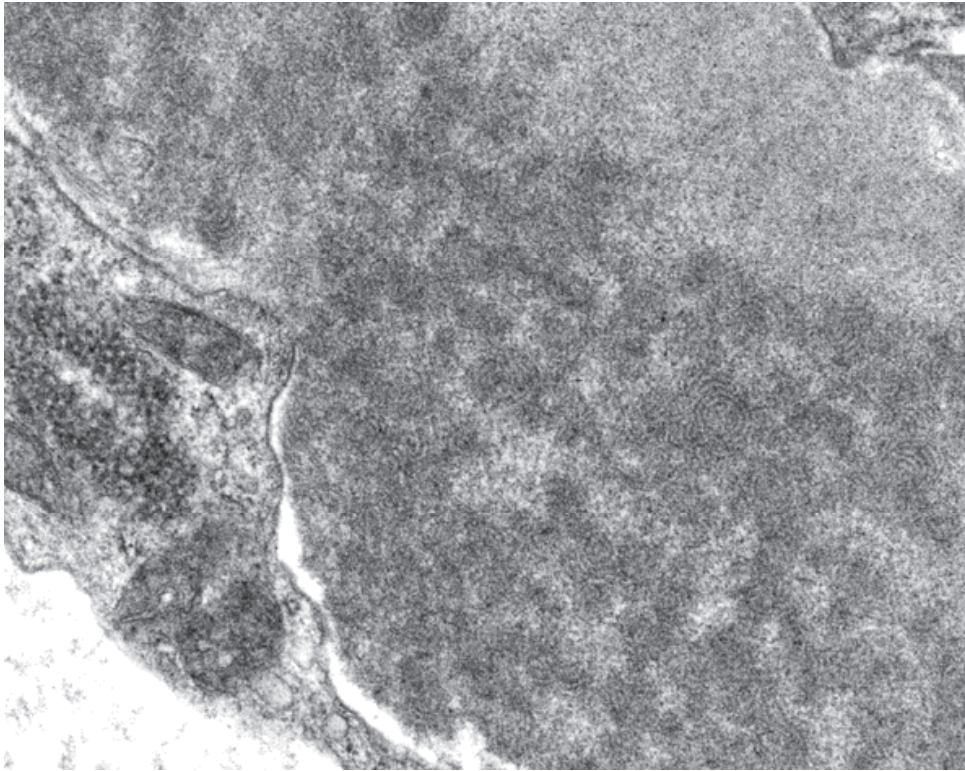


Fig. 11. Subendothelial concentric lamellae forming “finger prints”, in a case of lupus nephritis. OM: x12000.

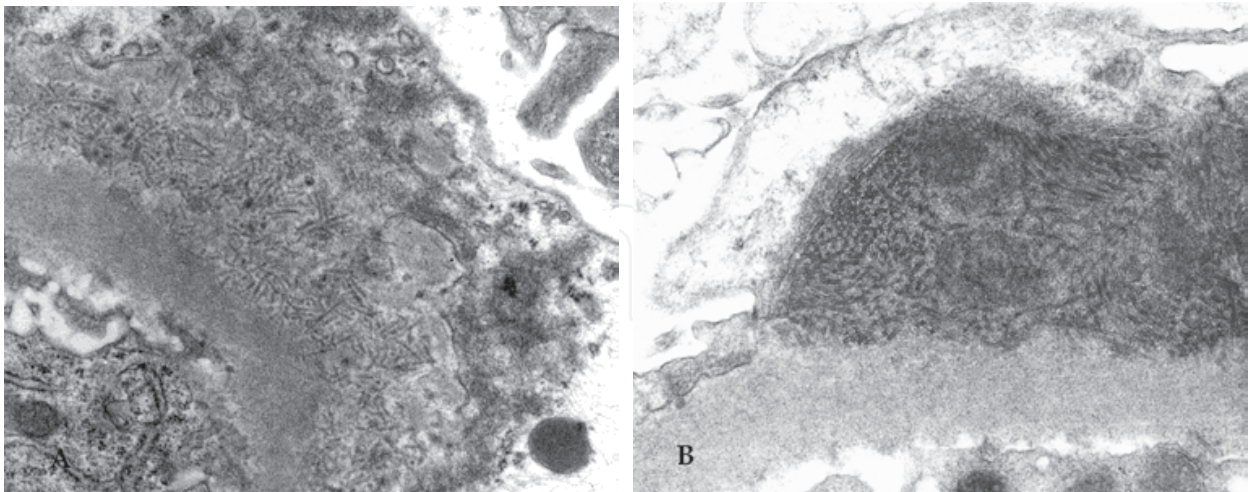


Fig. 12. A-B. Glomerular fibrillary (A, OM: x12000; Nebuloni, 2009) and immunotactoid (B, OM: x12000) immunodeposits in subepithelial position. Fibrillary deposits are composed by fibrils with a diameter less wide than 30nm, and they present a less ordered array than immunotactoid. The latter consist of microtubules, showing an hollow centre also at medium magnification.

Whereas most of structured deposits are easily distinguished from amyloid, fibrillar array in FGN may present various similarities with amyloid. FGN and ITG represent pathological entities characterized by the glomerular deposition of fibrillary/microtubular structures, whose identification is possible only by TEM. Rare cases of extraglomerular and extrarenal localization are also reported (Calle Ginestra et al., 1995; Adeyi et al., 2001; Sabatine et al., 2002). Pathologists generally maintain a conventional sub-structural distinction of FGN and ITG, based on diameters and random, or more ordered, arrangement of the fibrils. However, difference in clinicopathological correlation remain controversial (Alpers & Kowalewska, 2008; Schwartz et al., 2002). Clinical presentation in both varieties is nephrotic syndrome, with a tendency to early renal insufficiency. Because of the fact that cryoglobulins may present a similar morphology, definitive diagnosis generally include the exclusion of cryoglobulinemia by clinical analyses. In FGN, fibrils are Congo red negative, but present sub-structural similarities with amyloid fibrils. These include: a random arrangement, and, in rare cases, a wide range diameter, overlapping those of amyloid fibrils. Moreover, Yang et al. reported a case of Congo-red negative FGN with amyloid P associated to the fibrils, demonstrated by ITEM (Yang et al., 1992). However, in the majority of the cases of FGN, fibrils show a wider diameter than amyloid (range: 15-30). Amyloid fibrils have a more defined profile and generally a diameter smaller than 12nm. Amyloid ultrastructural appearance is sufficiently characteristic, so that the diagnosis of amyloidosis should continue to be considered even when Congo red staining is negative (Dember, 2006).

4.3 Glomerular immunocomplex diseases

The IF pattern of renal amyloidosis frequently shows glomerular deposition, including IgG, C3, IgA and IgM., the latter mainly in secondary AA. In fact, most cases of AA are associated to rheumatoid arthritis, which frequently presents an IgA and IgM glomerular deposition. In about one third of patient with AA, electron-dense IgA deposition in paramesangial areas may suggest a diagnosis of IgA nephropathy. TEM can easily prove the presence of unspecific immunocomplex in a context of amyloid deposition (Nishi et al., 2008; Yang & Gallo, 1990).

5. Ultrastructural detection of amyloid fibrils in non-conventional tissue preparations

In diagnostic practice, it happens that the need for ultrastructural analyses emerges after the results of histological examination on paraffin embedded tissue sections. In these cases, if there is no specific sample prepared for TEM, the residual formalin-fixed paraffin-embedded tissue can be recovered for ultrastructural analysis. Briefly, the retrieving of tissues from paraffin consists on various changes in paraffin solvent (i.e. xylene, or rather, its less toxic substitutes), followed by rehydration, using descending scale of ethanol, prior to the specific preparation procedures for TEM (i.e. fixation and resin embedding). Ultrastructural diagnoses on tissues retrieved from paraffin have been often used in various diagnostic fields (Tosoni et al., 2002). In our experience, in kidney diseases, it allows the identification of immunocomplex deposits with good maintenance of sensitivity. This latter depends mainly by a good primary fixation in buffered formalin. Small tissues fragments, prepared without mechanical stress, immediately immersed in fixative, have a good preservation of the sub-structural detail. It should be noted that, contrary to the setting of

glutaraldehyde fixation, formalin fixation for morphological studies is best carried out at room temperature. Ultrastructural general morphology of amyloid deposits of tissues retrieved from paraffin is conserved (Fig. 13).

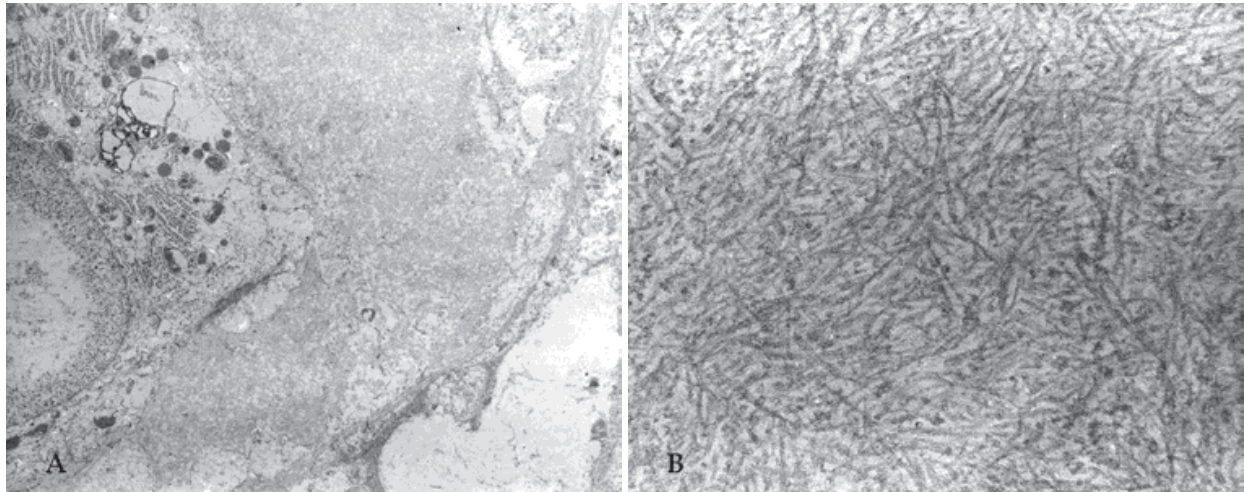


Fig. 13. A-B. Amyloid deposit in liver tissue retrieved from paraffin. Perisinusoidal space (A, OM x3000) is filled with a large amount of amyloid fibrils (B, x30000). The hepatocyte, on the left of panel A shows the relatively good sub-structural preservation after formalin fixation/paraffin embedding, and retrieving procedure.

Some authors report the possibility of change in fibrils diameter depending on formalin fixation (Sikorska et al., 2009), but fibrillar structure and aggregation patterns are maintained. Otherwise, sensitivity of TEM analysis may be reduced because of reduction in specificity. In fact, fibrillar ECM can appear more electrondense and can be difficult to distinguish from amyloid fibrils. Moreover, in the presence of poor preservation of cell's plasmalemma, intracytoplasmic intermediated filaments can mimic amyloid dense aggregates. Nevertheless, the presence of groups of randomly oriented non branched 10 nm fibrils is generally highly suspicious for amyloidosis. Our experience concerns mainly renal amyloidosis. TEM on renal biopsy retrieved from paraffin may be indicated in the following cases:

- Congo red positive /immunolabeling negative: TEM to confirm amyloidosis
- Clinical suspicion of renal amyloidosis, Congo red/immunolabeling with doubtful results: TEM to confirm amyloidosis
- Congo red positive, no glomeruli in frozen sections: TEM to evaluate concomitant immune-complex glomerulopathy

Amyloid can also be detected in frozen tissues residues retrieved for TEM after immunofluorescence. However, frozen tissues should be preferably stored, to devote to any successive typing analyses, if necessary (Picken, 2010).

6. Conclusion

Amyloid is a characteristic conformational status of various proteins in specific conditions, frequently associated with disease. Morphology of amyloid fibrils is distinctive and useful in the diagnosis of amyloidosis, also in the early stage of disease. ITEM can provide a high sensitive typing approach, specially in unusual or new amyloid forms.

7. References

- Adeyi, OA.; Sethi, S. & Rennke, HG. (2001). Fibrillary glomerulonephritis: a report of 2 cases with extensive glomerular and tubular deposits. *Hum Pathol*, Vol.32, No.6, (June 2001), pp. 660-663, ISSN 0046-8177
- Allsop, D.; Kidd, M.; Landon, M. & Tomlinson, A. (1986). Isolated senile plaque cores in Alzheimer's disease and Down's syndrome show differences in morphology. *J Neurol Neurosurg Psychiatry*, Vol.49, No.8, (August 1986), pp. 886-892, ISSN 0022-3050
- Alpers, CE. & Kowalewska, J. (2008). Fibrillary glomerulonephritis and immunotactoid glomerulopathy. *J Am Soc Nephrol*, Vol.19, No.1, (January 2008), pp. 34-37, ISSN 1046-6673
- Arbustini, E.; Verga, L.; Concardi, M.; Palladini, G.; Obici, L. & Merlini, G. (2002). Electron and immuno-electron microscopy of abdominal fat identifies and characterizes amyloid fibrils in suspected cardiac amyloidosis. *Amyloid*, Vol.9, No.2, (June 2002), pp. 108-114, ISSN 1350-6129
- Bély, M.; Kapp, P.; Szabó, TS.; Lakatos, T. & Apáthy, A. (2005). Electron microscopic characteristics of beta2-microglobulin amyloid deposits in long-term haemodialysis. *Ultrastruct Pathol*, Vol.29, No.6, (November-December 2005), pp. 483-491, ISSN 0191-3123
- Calls Ginesta, J.; Torras, A.; Ricart, MJ.; Ramirez, J.; Campo, E.; Darnell, A.; Andreu, J. & Revert, L. (1995). Fibrillary glomerulonephritis and pulmonary hemorrhage in a patient with renal transplantation. *Clin Nephrol*, Vol.43, No.3, (March 1995), pp. 180-183, ISSN 0301-0430
- Caubet, C.; Bousset, L.; Clemmensen, O.; Sourigues, Y.; Bygum, A.; Chavanas, S.; Coudane, F.; Hsu, CY.; Betz, RC.; Melki, R.; Simon, M. & Serre, G. (2010). A new amyloidosis caused by fibrillar aggregates of mutated corneodesmosin. *FASEB J*, Vol.24, No.9, (September 2010), pp. 3416-3426, ISSN 0892-6638
- Dember, LM. (2006). Amyloidosis-associated kidney disease. *J Am Soc Nephrol*, Vol.17, No.12, (December 2006), pp. 3458-3471, ISSN 1046-6673
- Dikman, SH.; Churg, J. & Kahn, T. (1981). Morphologic and clinical correlates in renal amyloidosis. *Hum Pathol*, Vol.12, No.2, (February 1981), pp. 160-169, ISSN 0046-8177
- Dzamba, BJ. & Peters, DM. (1991). Arrangement of cellular fibronectin in noncollagenous fibrils in human fibroblast cultures. *J Cell Sci.*, Vol.100, No.3, (November 1991), pp. 605-612, ISSN 0021-9533
- Fändrich M. (2007). On the structural definition of amyloid fibrils and other polypeptide aggregates. *Cell Mol Life Sci*, Vol.64, No.16, (August 2007), pp. 2066-78, ISSN 1420-682X
- Fändrich M, Meinhardt J, Grigorieff N. (2009). Structural polymorphism of Alzheimer Aβ and other amyloid fibrils. *Prion*, Vol.3, No.2, (April 2009), pp. 89-93, ISSN 1933-6896
- Fournier, JG.; Escaig-Haye, F. & Grigoriev, V. (2000). Ultrastructural localization of prion proteins: physiological and pathological implications. *Microsc Res Tech*, Vol.50, No.1, (July 2000), pp.76-88, ISSN 1059-910X
- Friedrich RP, Tepper K, Röncke R, Soom M, Westermann M, Reymann K, Kaether C, Fändrich M. (2010). Mechanism of amyloid plaque formation suggests an

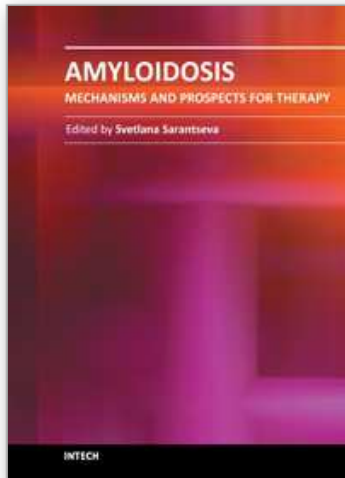
- intracellular basis of Abeta pathogenicity. *Proc Natl Acad Sci U S A*, Vol.107, No.5, (February 2010), pp. 1942-1947, ISSN 0027-8424
- Gellermann, GP.; Appel, TR.; Tannert, A.; Radestock, A.; Hortschansky, P.; Schroeckh, V.; Leisner, C.; Lütkepohl, T.; Shtrasburg, S.; Röcken, C.; Pras, M.; Linke, RP.; Diekmann, S. & Fändrich, M. (2005). Raft lipids as common components of human extracellular amyloid fibrils. *Proc Natl Acad Sci U S A*, Vol.102, No.18, (May 2005), pp. 6297-6302, ISSN 0027-8424
- Greenwald, J. & Riek, R. (2010). Biology of amyloid: structure, function, and regulation. *Structure*, Vol.18, No.10, (October 2010), pp. 1244-1260, ISSN 0969-2127
- Inoue, S.; Kuroiwa, M.; Ohashi, K.; Hara, M. & Kisilevsky, R. (1997). Ultrastructural organization of hemodialysis-associated beta 2-microglobulin amyloid fibrils. *Kidney Int*, Vol.52, No.6, (December 1997), pp. 1543-1549, ISSN 0085-2538
- Inoue, S.; Kuroiwa, M.; Saraiva, MJ.; Guimarães, A. & Kisilevsky, R. (1998). Ultrastructure of familial amyloid polyneuropathy amyloid fibrils: examination with high-resolution electron microscopy. *J Struct Biol*, Vol.124, No.1, (December 1998), pp. 1-12, ISSN 1047-8477
- Inoue, S.; Kuroiwa, M. & Kisilevsky, R. (1999). Basement membranes, microfibrils and beta amyloid fibrillogenesis in Alzheimer's disease: high resolution ultrastructural findings. *Brain Res Rev*, Vol.29, No.2-3, (April 1999), pp. 218-31, ISSN 006-8993
- Jadoul M, Garbar C, van Ypersele de Strihou C. (2001). Pathological aspects of beta(2)-microglobulin amyloidosis. *Semin Dial*, Vol.14, No.2, (March-April 2001), pp. 86-89, ISSN 0894-0959
- Jiménez, JL.; Tennent, G.; Pepys, M. & Saibil, HR. (2001). Structural diversity of ex vivo amyloid fibrils studied by cryo-electron microscopy. *J Mol Biol*, Vol.311, No.2, (August 2001), pp. 241-247, ISSN 0022-2836
- Joh, K. Pathology of glomerular deposition disease. (2007). *Pathol Int*, Vol.57, No.9, (September 2007), pp. 551-565, ISSN 1320-5463
- Kaye, GC.; Butler, MG.; D'Ardenne, AJ.; Edmondson, SJ.; Camm, AJ. & Slavin, G. (1986). Identification of immunoreactive atrial natriuretic peptide in atrial amyloid. *J Clin Pathol*, Vol.39, No.5, (May 1986), pp. 581-582, ISSN 00219746
- Keeling, J.; Teng, J. & Herrera, G. (2004). AL-amyloidosis and light-chain deposition disease light chains induce divergent phenotypic transformations of human mesangial cells. *Laboratory Investigation*, Vol.84, (August 2004), pp. 1322-1338, ISSN 0023-6837
- King, JA.; Culpepper, RM.; Corey, GR.; Tucker, JA.; Lajoie, G. & Howell, DN. (2000). Glomerulopathies with fibrillary deposits. *Ultrastruct Pathol*, Vol.24, No.1, (January-February 2000), pp. 15-21, ISSN 0191-3123
- Kluve-Beckerman, B.; Liepnieks, JJ.; Wang, L. & Benson, MD. (1999). A cell culture system for the study of amyloid pathogenesis. Amyloid formation by peritoneal macrophages cultured with recombinant serum amyloid A. *Am J Pathol*, Vol.155, No.1, (July 1999), pp. 123-133, ISSN 0002-9440
- Korbet SM, Schwartz MM, Lewis EJ. (1994). The fibrillary glomerulopathies. *Am J Kidney Dis*, Vol.23, No.5, (May 1994), pp. 751-765, ISSN 0272-6386
- Kronz, JD.; Neu, AM. & Nadasdy, T. (1998). When nonconglomerular glomerular fibrils do not represent fibrillary glomerulonephritis: nonspecific mesangial fibrils in sclerosing glomeruli. *Clin Nephrol*, Vol.50, No.4, (October 1998), pp. 218-223, ISSN 0301-0430

- Leonhardt, RM.; Vigneron, N.; Rahner, C.; Van den Eynde, BJ. & Cresswell, P. (2010). Endoplasmic reticulum export, subcellular distribution, and fibril formation by Pmel17 require an intact N-terminal domain junction. *J Biol Chem*, Vol.285, No.21, (May 2010), pp. 16166-16183, ISSN 0021-9258
- Makin, OS. & Serpell, LC. (2005). Structures for amyloid fibrils. *FEBS J*, Vol.272, No.23, (December 2005), pp. 5950-61, ISSN 1742-464X
- Merlini, G. & Bellotti, V. (2003). Molecular mechanisms of amyloidosis. *N Engl J Med*, Vol.349, No.6, (August 2003), pp. 583-96, ISSN 0028-4793
- Morten, IJ.; Gosal, WS.; Radford, SE. & Hewitt, EW. (2007). Investigation into the role of macrophages in the formation and degradation of beta2-microglobulin amyloid fibrils. *J Biol Chem*, Vol.282, No.40, (October 2007), pp. 29691-29700, ISSN 0021-9258
- Nebuloni, M.; Genderini, A.; Tosoni, A.; Caruso, S. & Barbiano di Belgiojoso, G. (2009). Fibrillary glomerulonephritis with prevalent IgA deposition associated with undifferentiated connective tissue disease: a case report. *NDT Plus*, Vol.3, pp. 57-59, ISSN 0931-0509
- Nishi S, Alchi B, Imai N, Gejyo F. (2008). New advances in renal amyloidosis. *Clin Exp Nephrol*, Vol.12, No.2, (April 2008), pp. 93-101
- Pan, KM.; Baldwin, M.; Nguyen, J.; Gasset, M.; Serban, A.; Groth, D.; Mehlhorn, I.; Huang, Z.; Fletterick, RJ. & Cohen, FE. (1993) Conversion of alpha-helices into beta-sheets features in the formation of the scrapie prion proteins. *Proc Natl Acad Sci U S A*, Vol.90, No.23, (December 1993), pp. 10962-10966, ISSN 0027-8424
- Pedersen, JS.; Andersen, CB. & Otzen, DE. (2010). Amyloid structure--one but not the same: the many levels of fibrillar polymorphism. *FEBS J*, Vol.277, No.22, (November 2010), pp. 4591-4601, ISSN 1742-464X
- Pettersson, T. & Konttinen, YT. (2010). Amyloidosis-recent developments. *Semin Arthritis Rheum*, Vol.39, No.5, (April 2010), pp. 356-68, ISSN 0049-0172
- Picken, MM. & Linke, RP. (2009). Nephrotic syndrome due to an amyloidogenic mutation in fibrinogen A alpha chain. *J Am Soc Nephrol*, Vol.20, No.8, (August 2009), pp. 1681-1685, ISSN 1046-6673
- Picken, MM. (2010). Amyloidosis-where are we now and where are we heading?. *Arch Pathol Lab Med*, Vol.134, No.4, (April 2010), pp. 545-551, ISSN 0003-9985
- Prusiner, SB. (1998). The prion diseases. *Brain Pathol*, Vol.8, No.3, (July 1998), pp. 499-513, ISSN 1015-6305
- Rozemuller, AJ.; Roos, RA.; Bots, GT; Kamphorst, W.; Eikelenboom, P. & Van Nostrand, WE. (1993). Distribution of beta/A4 protein and amyloid precursor protein in hereditary cerebral hemorrhage with amyloidosis-Dutch type and Alzheimer's disease. *Am J Pathol*, Vol.142, No. 5, (May 1993), pp. 1449-1457, ISSN 0002-9440
- Sabatine, MS.; Aretz, HT.; Fang, LS. & Dec, GW. Images in cardiovascular medicine. Fibrillary/immunotactoid glomerulopathy with cardiac involvement. *Circulation*, Vol.105, No.15, (April 2002), e120-1, ISSN 0009-7322
- Sachse C, Xu C, Wieligmann K, Diekmann S, Grigorieff N, Fändrich M. (2006). Quaternary structure of a mature amyloid fibril from Alzheimer's Abeta(1-40) peptide. *J Mol Biol*, Vol.362, No.2, (September 2006), pp. 347-354, ISSN 0022-2836
- Santostefano, M.; Zanchelli, F.; Zaccaria, A.; Poletti, G. & Fusaroli, M. (2005). The ultrastructural basis of renal pathology in monoclonal gammopathies. *J Nephrol*, Vol.18, No.6, (November-December 2005), pp. 659-675, ISSN 1121-8428

- Schreml, S.; Szeimies, RM.; Vogt, T.; Landthaler, M.; Schroeder, J. & Babilas, P. (2010). Cutaneous amyloidoses and systemic amyloidoses with cutaneous involvement. *Eur J Dermatol*, Vol.20, No.2, (March-April 2010), pp. 152-160, ISSN 1167-1122
- Schwartz, MM.; Korbet, SM. & Lewis, EJ. (2002). Immunotactoid glomerulopathy. *J Am Soc Nephrol*, Vol.13, No.5, (May 2002), pp. 1390-1397, ISSN 1046-6673
- Sen, S. & Sarsik, B. (2010). A proposed histopathologic classification, scoring, and grading system for renal amyloidosis: standardization of renal amyloid biopsy report. *Arch Pathol Lab Med*, Vol.134, No.4, (April 2010), pp. 532-544, ISSN 0003-9985
- Serpell, LC. (2000). Alzheimer's amyloid fibrils: structure and assembly. *Biochim Biophys Acta*, Vol.1502, No.1 (July 26), pp. 16-30, ISSN 0304-4165
- Sherratt, MJ.; Wess, TJ.; Baldock, C.; Ashworth, J.; Purslow, PP.; Shuttleworth, CA. & Kielty, CM. (2001). Fibrillin-rich microfibrils of the extracellular matrix: ultrastructure and assembly. *Micron*, Vol.32, No.2, (February 2001), pp. 185-200, ISSN 0968-4328
- Sikorska, B.; Liberski, PP.; Sobów, T.; Budka, H. & Ironside, JW. (2009). Ultrastructural study of florid plaques in variant Creutzfeldt-Jakob disease: a comparison with amyloid plaques in kuru, sporadic Creutzfeldt-Jakob disease and Gerstmann-Sträussler-Scheinker disease. *Neuropathol Appl Neurobiol*, Vol.35, No.1, (February 2009), pp. 46-59, ISSN 0305-1846
- Sipe, JD.; Benson, MD.; Buxbaum, JN.; Ikeda, S.; Merlini, G.; Saraiva, MJ. & Westermark, P. (2010). Amyloid fibril protein nomenclature: 2010 recommendations from the nomenclature committee of the International Society of Amyloidosis. *Amyloid*, Vol.17, No.3-4, (September 2010), pp. 101-4, ISSN 1350-6129
- Sipe, JD. & Cohen, AS. (2000). Review: history of the amyloid fibril. *J Struct Biol*, Vol.130, No.2-3, (June 2000), pp. 88-98, ISSN 1047-8477
- Stromer, T. & Serpell, LC. (2005). Structure and morphology of the Alzheimer's amyloid fibril. *Microsc Res Tech*, Vol.67, No.3-4, (July 2005), pp. 210-217, ISSN 1059-910X
- Teng, J.; Russell, WJ.; Gu, X.; Cardelli, J.; Jones, ML. & Herrera, GA. (2004). Different types of glomerulopathic light chains interact with mesangial cells using a common receptor but exhibit different intracellular trafficking patterns. *Lab Invest*, Vol.84, No.4, (April 2004), pp. 440-451, ISSN 0023-6837
- Tosoni, A.; Nebuloni, M.; Ferri, A.; Bonetto, S.; Antinori, S.; Scaglia, M.; Xiao, L.; Moura, H.; Visvesvara, GS.; Vago, L. & Costanzi, G. (2002). Disseminated microsporidiosis caused by *Encephalitozoon cuniculi* III (dog type) in an Italian AIDS patient: a retrospective study. *Mod Pathol*, Vol.15, No.5, (May 2002), pp. 577-583, ISSN 0893-3952
- Vallat, JM.; Magy, L.; Richard, L.; Sturtz, F. & Couratier, P. (2008). Contribution of electron microscopy to the study of neuropathies associated with an IgG monoclonal paraproteinemia. *Micron*, Vol.39, No.2, (January 2007), pp. 61-70, ISSN 0968-4328
- Weber, E.; Rossi, A.; Solito, R.; Sacchi, G.; Agliano, M. & Gerli, R. (2002). Focal adhesion molecules expression and fibrillin deposition by lymphatic and blood vessel endothelial cells in culture. *Microvasc Res*, Vol.64, No.1, (July 2002), pp. 47-55, ISSN 0026-2862
- Westermark, P.; Davey, E.; Lindbom, K. & Enqvist, S. (2006). Subcutaneous fat tissue for diagnosis and studies of systemic amyloidosis. *Acta Histochem*, Vol.108, No.3, (May 2006), pp. 209-213, ISSN 0065-1281

- Yazawa H, Yu ZX, Takeda, Le Y, Gong W, Ferrans VJ, Oppenheim JJ, Li CC, Wang JM. (2001). Beta amyloid peptide (Abeta42) is internalized via the G-protein-coupled receptor FPRL1 and forms fibrillar aggregates in macrophages. *FASEB J*, Vol.15, No.13, (November 2001), pp. 2454-2462, ISSN 0892-6638
- Yamaguchi, H; Nakazato, Y.; Hirai, S.; Shoji, M. & Harigava, Y. (1989). Electron micrograph of diffuse plaques. Initial stage of senile plaque formation in the Alzheimer brain. *Am J Pathol*, Vol.135, No.4, (October 1989), pp.593-597, ISSN 0002-9440
- Yang, GC. & Gallo, GR. (1990). Protein A-gold immunoelectron microscopic study of amyloid fibrils, granular deposits, and fibrillar luminal aggregates in renal amyloidosis. *Am J Pathol*, Vol.137, No.5, (November 1990), pp. 1223-1231, ISSN 0002-9440
- Yang GC, Nieto R, Stachura I, Gallo G. (1992). Ultrastructural immunohistochemical localization of polyclonal IgG, C3, and amyloid P component on the Congo red-negative amyloid-like fibrils of fibrillary glomerulopathy. *Am J Pathol*, Vol.141, No.2, (August 1992), pp. 409-419, ISSN 0002-9440

IntechOpen



Amyloidosis - Mechanisms and Prospects for Therapy

Edited by Dr. Svetlana Sarantseva

ISBN 978-953-307-253-1

Hard cover, 216 pages

Publisher InTech

Published online 22, September, 2011

Published in print edition September, 2011

Amyloidoses are a heterogeneous group of diverse etiology diseases. They are characterized by an endogenous production of abnormal proteins called amyloid proteins, which are not hydrosoluble, form depots in various organs and tissue of animals and humans and cause dysfunctions. Despite many decades of research, the origin of the pathogenesis and the molecular determinants involved in amyloid diseases has remained elusive. At present, there is not an effective treatment to prevent protein misfolding in these amyloid diseases. The aim of this book is to present an overview of different aspects of amyloidoses from basic mechanisms and diagnosis to latest advancements in treatment.

How to reference

In order to correctly reference this scholarly work, feel free to copy and paste the following:

Tosoni A., Barbiano di Belgiojoso G. and Nebuloni M. (2011). Electron Microscopy in the Diagnosis of Amyloidosis, *Amyloidosis - Mechanisms and Prospects for Therapy*, Dr. Svetlana Sarantseva (Ed.), ISBN: 978-953-307-253-1, InTech, Available from: <http://www.intechopen.com/books/amyloidosis-mechanisms-and-prospects-for-therapy/electron-microscopy-in-the-diagnosis-of-amyloidosis>

INTECH
open science | open minds

InTech Europe

University Campus STeP Ri
Slavka Krautzeka 83/A
51000 Rijeka, Croatia
Phone: +385 (51) 770 447
Fax: +385 (51) 686 166
www.intechopen.com

InTech China

Unit 405, Office Block, Hotel Equatorial Shanghai
No.65, Yan An Road (West), Shanghai, 200040, China
中国上海市延安西路65号上海国际贵都大饭店办公楼405单元
Phone: +86-21-62489820
Fax: +86-21-62489821

© 2011 The Author(s). Licensee IntechOpen. This chapter is distributed under the terms of the [Creative Commons Attribution-NonCommercial-ShareAlike-3.0 License](#), which permits use, distribution and reproduction for non-commercial purposes, provided the original is properly cited and derivative works building on this content are distributed under the same license.

IntechOpen

IntechOpen